

AIRBORNE SPECTROPHOTOMETRY OF η CARINAE FROM 4.5 TO 7.5 MICRONS AND A MODEL FOR SOURCE MORPHOLOGY

RAY W. RUSSELL, DAVID K. LYNCH, JOHN A. HACKWELL,¹ RICHARD J. RUDY, AND GEORGE S. ROSSANO
 The Aerospace Corporation, Space Sciences Laboratory

AND

M. W. CASTELAZ^{1,2}

Space Science Division, NASA/Ames Research Center

Received 1986 September 4; accepted 1987 March 6

ABSTRACT

Spectrophotometric observations of η Car between 4.5 and 7.5 μm show a featureless thermal-like spectrum with no fine-structure lines or broad emission or absorption features. The color temperature of the spectrum is approximately 375 K. We observe silicate emission at 10.5 μm at $\sim 6 \times 10^{-14} \text{ W cm}^{-2} \mu\text{m}^{-1}$, which exceeds the extrapolated gray-body curve by a factor of about 2. High spatial resolution maps at 3.5, 4.8, and 10 μm obtained from the ground are used to discuss the dust distribution and temperature structure, and to present a model for general source morphology. The upper limit to the brightness of the [Ar II] fine-structure emission line at 6.98 μm is $< 7 \times 10^{-16} \text{ W cm}^{-2}$, which still allows for a significant overabundance of argon and is consistent with the evolved nature of the source.

Subject headings: infrared: spectra — nebulae: abundances — nebulae: individual (η Carinae) — spectrophotometry

I. INTRODUCTION

Eta Carinae first received astrophysical attention between 1836 and 1847, when it brightened from around first magnitude to -1 mag, making it the second brightest star in the sky (Herschel 1847). During the outburst it apparently ejected a large shell, which subsequently cooled and condensed dust grains which obscured the central star. An interesting and beautiful general discussion has recently been presented by Malin (1987). The shell is elongated ($12'' \times 18''$), irregular, and polarized in the visible (Warren-Smith *et al.* 1979) and is said to resemble a little man or "homunculus" (Gaviola 1950). In 1968, Neugebauer and Westphal found this object to be an intense source of infrared radiation. Westphal and Neugebauer (1969) showed that there was a broad-band emission feature at 10 μm , later attributed to emission from silicate grains (Robinson, Hyland, and Thomas 1973). The infrared nebula is similar in size to its optical counterpart ($12'' \times 18''$; see Aitken and Jones 1975; Hackwell, Gehrz, and Grasdalen 1986, hereafter HGG). Currently, η Car is the brightest stellar source in the sky at both 10 and 20 μm , though it is somewhat variable (Whitelock *et al.* 1983), and now has a visible brightness of ~ 6.2 mag.

We report the first measurements of η Car between 4.5 and 7.5 μm , a spectral region accessible only from airborne telescopes or space, and discuss the source morphology in light of new ground-based maps obtained from the Southern Hemisphere.

II. INSTRUMENTATION

The instrument used to obtain all of the spectral data was a single-channel liquid helium-cooled circular variable filter

¹ Visiting Astronomer, Cerro Tololo Inter-American Observatory, which is operated by Associated Universities for Research in Astronomy, Inc., under contract to the National Science Foundation.

² National Academy of Sciences/National Research Council Research Fellowship.

(CVF) spectrophotometer. Four broad-band filters and three sector wheels with a wedge-shaped cross section provide continuously variable wavelength transmission and lie in a single filter wheel which is driven by a stepper motor controller external to the Dewar. The CVFs are multilayer dielectric interference filters cooled to about 10 K which transmit 2.5–4.5 μm , 4–8 μm , and 8–14 μm , respectively; the bandpass is roughly 3% of the wavelength. The detector is a Si:Ga photoconductor which was operated under background-limited conditions when viewing through the 4–8 μm wedge or through the 10.5 μm broad-band filter, as was the case for all the data presented here.

III. OBSERVATIONS

a) Spectrophotometry

Spectrophotometric observations of η Car (Fig. 1) were made on the refurbished NASA/Ames Learjet Observatory (LJO) 12" altazimuth telescope at the f/6.5 Cassegrain focus (Russell 1984). All measurements were made in the standard dual beam mode using the chopping secondary with a beam throw of 11' in the cross elevation direction and a chopping frequency of 33 Hz. A 2 mm entrance aperture gave an aperture diameter of ~ 3.5 . Guiding was done via a 4 inch (10 cm) diameter bore-sighted guide telescope whose output was fed into an intensified low-light level TV via a fiber optic bundle. The TV signal is used by the computer-controlled tracker to maintain stabilized pointing from the aircraft. All of the observations were made from the Kwajalein Missile Range (N8°43', E167°43'). We flew at 12.5–13.7 km, so at no time were we above the tropopause (~ 16.8 km). The object η Car was observed several nights between 1986 March 16 and April 25, though we report here only the best spectrum taken April 24 (turbulence and high clouds degraded the quality of several nights' data). The Moon and α Ori were used as calibration sources. The star α Ori was observed episodically during the same period, and the Moon was observed on 1986 March 16.

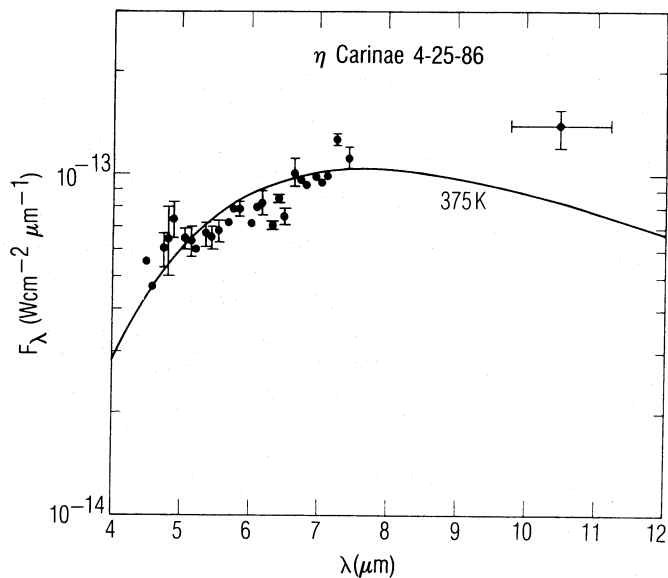


FIG. 1.—Spectrum of η Car measured from 4.5 to 7.5 μm . The spectrum exhibits a featureless thermal continuum consistent with gray-body emission at about 375 K.

Videotapes of the tracked position on the Moon were used in conjunction with the maps from Saari and Shorthill (1967) to derive the temperature of the positions observed. The absolute calibration from α Ori and the Moon agree to 20%.

b) Infrared Maps

The data used to produce the infrared maps shown in Figures 2 and 3 were obtained with the CTIO bolometer system mounted on the 4 m telescope. The fast-mapping technique used here has been described in detail by Hackwell and Schweizer (1983) and by HGG. In brief, the computer-controlled secondary mirror is stepped in declination while chopping north-south. The signal is sampled digitally, and the intensity at each pixel is taken to be the difference between the signal on the source and the displaced “sky” beam. Once a declination scan is completed, the telescope is offset by one pixel in right ascension to build a two-dimensional image. For these measurements, the entrance aperture was 1 mm, which gives a beam diameter of about $1''.8$, the chopper “throw” was $30''$ at 10 Hz, the pixel spacing was $0''.5$, and each map was 48×48 pixels ($24'' \times 24''$). The $30''$ throw was sufficient to ensure that there was less than 0.4% of the peak signal in the reference beam.

The data shown in Figure 2 were taken during 1984 April. Each of the η Car images (Figs. 2a–2c) was made by aligning and co-adding two scans of the object to reduce systematic errors caused by seeing and guiding. Calibration of the images was done by mapping the stars α Sco (4.8 and 10 μm), γ Cru (3.5, 4.8, and 10 μm), and BS 6136 (3.5 μm) using the same chopper throw and pixel spacing as for η Car.

The point-spread function shown in Figure 2d is the result of adding six scans of bright calibration stars made at 3.5, 4.8, and 10 μm . Because each wavelength was observed through the same entrance aperture and diffraction effects were minimal, we found that the size and shape of the point-spread function are independent of wavelength and circular in shape, but with a slight elongation in the chopping direction at the lowest intensity levels.

IV. DISCUSSION

The spectrum of η Car from 4.5 to 7.5 μm (Fig. 1) is most noteworthy for the absence of any spectral features. When the level and slope of the data shown here are compared with those interpolated from earlier ground-based observations at shorter and longer wavelengths, there is excellent agreement (Robinson, Hyland, and Thomas 1973; Joyce 1975; Aitken and Jones 1975). As the emission from 2 to 8 μm appears to be thermal in origin and there are no spectral features present in our data, we computed the dust color temperature by fitting the 4.5–7.5 μm data to a blackbody (i.e., emissivity independent of wavelength). The best visual fit to the data was obtained for a temperature of 375 K, as shown in Figure 1. By formally minimizing the χ^2 per degree of freedom, we obtained a best-fit temperature of 385 K with a reduced χ^2 of 4.2. This high value of χ^2 probably indicates that a single color temperature does not adequately model the dust emission even in the narrow spectral interval used here; a color temperature of over 600 K is derived from measurements at wavelengths shorter than 4.5 μm . Our result does indicate the presence of significant amounts of dust at temperatures between 350 and 400 K. Further evidence for this concept of the source morphology will be discussed later in the context of the ground-based maps. Although our 4.5–7.5 μm data agree well with earlier published results, our measurement of the 10.5 μm broad-band flux ($1.4 \times 10^{-13} \text{ W cm}^{-2} \mu\text{m}^{-1}$) is only about 75% of the average value quoted by the above-mentioned authors. We believe that the difference of $\sim 4 \times 10^{-14} \text{ W cm}^{-2} \mu\text{m}^{-1}$ is significant. Whitelock *et al.* (1983) have shown that η Car slowly brightened (and presumably is still brightening) in the visible and near-IR. They interpret the brightening as being due to an increasing flux from the embedded source which would be expected to result in an increase in the flux at longer wavelengths as well. Alternatively, the visible brightening could be due to a shell expanding and thinning, resulting in grains being farther from the star and cooler. This latter mechanism would thus cause a decrease in the flux at longer wavelengths which is dominated by thermal emission from extended regions of dust, as discussed below. Since the 4–8 μm fluxes have not changed by more than 10% in the last 15 years, it is surprising to find a 30% decrease in the 10.5 μm silicate emission during the same period, especially because our large aperture should pick up any outlying 10.5 μm flux. Further monitoring of the spectrum of the source will be required to clarify this issue.

exhibited by η Car from 1.0 to 2.3 μm (Allen, Jones, and Hyland 1985) and the evolved nature of the source, one might expect significant emission from [Ar II] at 6.98 μm . The species Ar I and Ar II should be the dominant forms of Ar based on the presence of [Fe II] and [Fe III] lines in the near-infrared. However, the dust continuum is rising very steeply from 2 to $\sim 9 \mu\text{m}$ (e.g., Gehrz *et al.* 1973) and provides a real impediment to the detection of line emission by a low spectral resolution instrument such as a CVF, which is geared to the study of dust features. We have derived an upper limit on [Ar II] emission from the data in Figure 1 to be $7 \times 10^{-16} \text{ W cm}^{-2}$. This upper limit corresponds to an abundance relative to hydrogen of 4.8×10^{-4} by number, using the intensity of Br γ from Allen, Jones, and Hyland (1985) of $\sim 1.3 \times 10^{-16} \text{ W cm}^{-2}$. The emissivities of the hydrogen lines are taken from Brocklehurst (1971) and Giles (1977) for $n_e \sim 10^4 \text{ cm}^{-3}$ and $T_e \sim 10^4 \text{ K}$. (Varying n_e from 10^3 to 10^5 cm^{-3} changes the result by $< 10\%$,

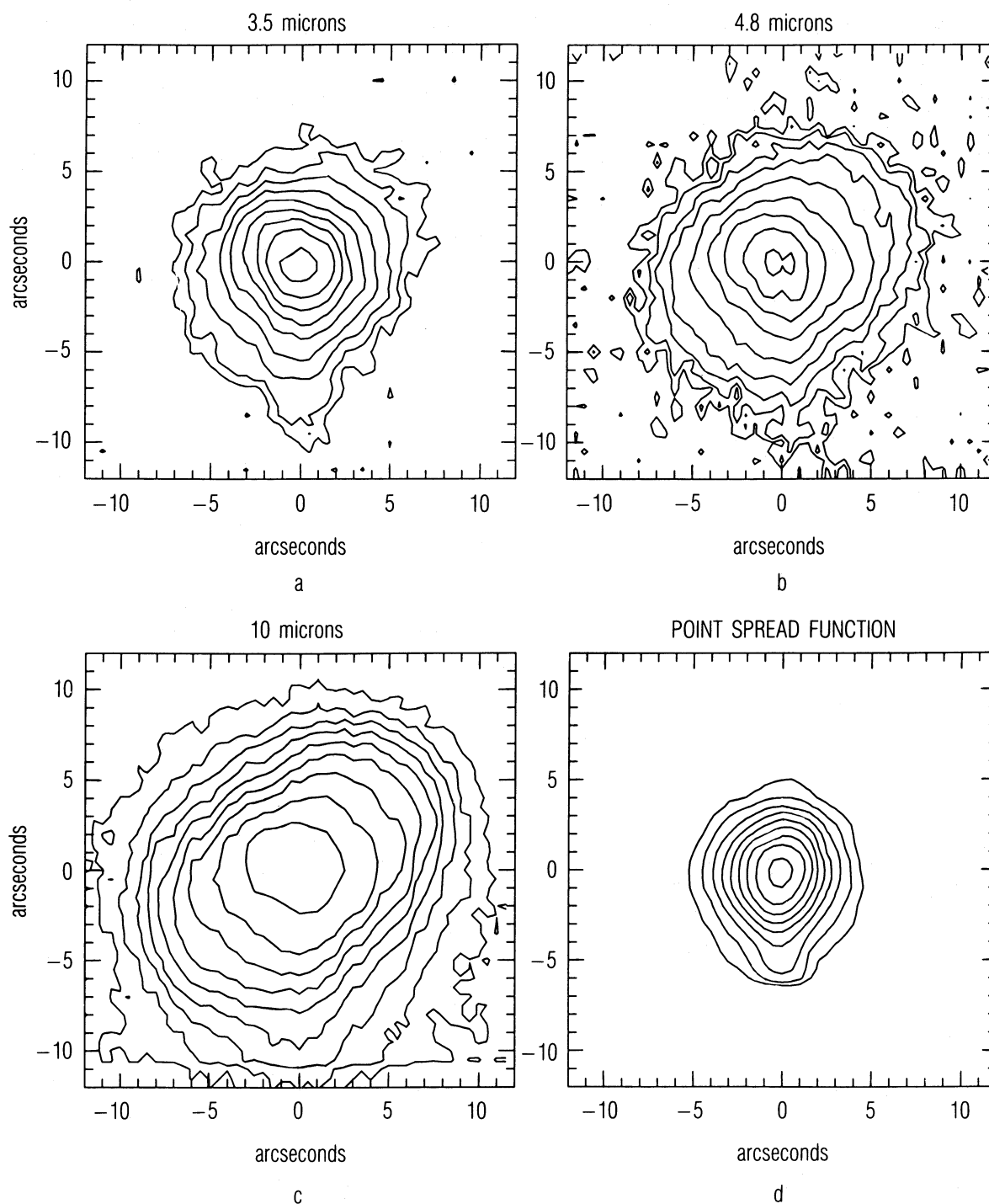


FIG. 2.—Images of η Car at (a) 3.5, (b) 4.8, and (c) 10 μm are compared with (d) the image of a bright star (the “point-spread function”). Note that η Car is significantly extended at all wavelengths compared with the star. North is up, and east is to the left. On all of the images, including (d), each contour level is a factor of 2 below the next highest contour; the innermost contours are at 80% of the peak surface brightness. On the 3.5 μm map, the innermost contour is at 90 Jy arcsec^{-2} ; on the 4.8 μm map the innermost contour is at 330 Jy arcsec^{-2} , and on the 10 μm map the innermost contour is at 560 Jy arcsec^{-2} .

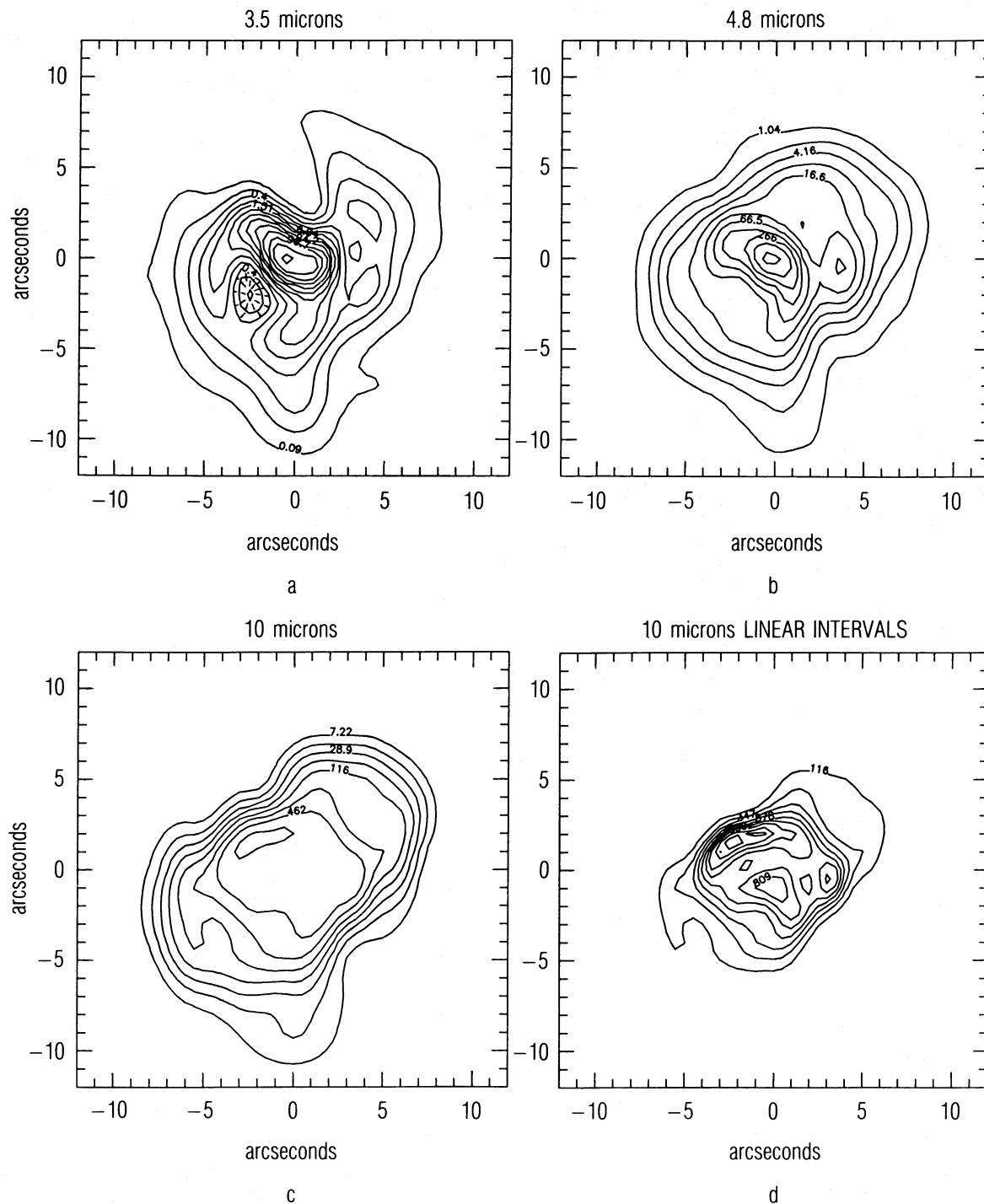


FIG. 3.—Results of applying a maximum entropy image restoration to the data shown in Fig. 2. In (a)–(c) the contour levels are spaced by a factor of 2 in surface brightness, and the innermost contour is at 80% of the peak surface brightness. On the $3.5\ \mu\text{m}$ map the innermost contour is at $390\ \text{Jy arcsec}^{-2}$, on the $4.8\ \mu\text{m}$ map the innermost contour is at $1060\ \text{Jy arcsec}^{-2}$, and on the $10\ \mu\text{m}$ map the innermost contour is at $920\ \text{Jy arcsec}^{-2}$. On all of the maps north is up and east is to the left. Note the northeast-southwest asymmetry in the core of the 3.5 and $4.8\ \mu\text{m}$ maps and the large extent of the $10\ \mu\text{m}$ core relative to that at 3.5 and $4.8\ \mu\text{m}$. In (d) the $10\ \mu\text{m}$ data are displayed with linearly spaced contours at 0.9, 0.8, 0.7, 0.6, 0.5, 0.4, 0.3, 0.2, and 0.1 of the peak intensity. Note the complex triple structure and the relatively large spacing of the individual components.

and T_e variations from 10^3 to 10^5 K result in $\lesssim 20\%$ changes.) The derived abundance upper limit of 8.68 on a scale where hydrogen = 12.00 is ~ 100 times the value of 6.6 cited by Cameron and Allen (1984), or the value of 6.8 quoted by Allen (1973). Thus, our result is readily seen to be consistent with the evolved nature of η Car and with the presence of numerous heavy-element lines in the near-infrared.

In view of the evolved nature of the source and the evidence for expulsion of dust and gas, one might expect to find broad emission features at 6.2 and 7.7 μm similar to those seen in other evolved sources such as NGC 7027 (Russell, Soifer, and Willner 1977). This expectation is strengthened because the emission at 10 μm is thin enough to exhibit a characteristic silicate emission profile (HGG). The opacity of the 6.2 and 7.7 μm features has not been observed to be greater than that of the strong silicate resonance at ~ 10 μm . Therefore, because optically thin silicate emission is observed at ~ 10 μm (HGG), the weaker features at 6.2 and 7.7 μm should also be optically thin and observable as well. There are two possible explanations for the absence of the 6.2 and 7.7 μm features. Either the grains are of the wrong composition to produce these features, or there is a second population of optically thick grains that is spatially distinct from the silicate grains and gives rise to the 4–8 μm continuum emission.

If the shells thrown off by the central star had contained sufficient mass, there might have been absorption features near 6.0 and 6.8 μm in the spectrum similar to those seen in several dense sources such as W33A (Willner *et al.* 1980). It has recently been shown that such absorption can be explained either by silicates (Hecht *et al.* 1986) or by carbon-rich grains (Tielens *et al.* 1984). However, large line-of-sight dust densities are needed to give 6.0 and 6.8 μm absorptions, and such large densities should produce a 10 μm silicate absorption feature which is neither observed nor indicated by model fits (e.g., HGG). It could be argued that silicates form a separate population of grains from those which produce the 6.0 and 6.8 μm absorptions observed in other sources, and that the shell ejecta should still be seen in absorption. However, the total extinction A_v to the gas emitting the near-infrared lines (i.e., extinction due to both interstellar matter and the extended shell ejecta) is currently estimated at only ~ 4 mag (Allen, Jones, and Hyland 1985); thus it is unlikely that extinction features would be seen in the mid-IR as a result of the ejecta alone.

Where is the dust which is emitting in the 4–8 μm spectral region, and what is its composition? Figures 2a–2c show that η Car is extended compared with a point source at all wavelengths, but that the contrast between the central core and the outer “homunculus” is greatest at the shortest wavelengths. This is in essential agreement with the results presented by Hyland *et al.* (1979) and by Mitchell *et al.* (1983), who scanned η Car at 2.2, 3.6, 8.4, 10.2, and 11.2 μm using a 1".1 FWHM beam. Although our beam diameter was larger, our data have a lower limiting surface brightness than theirs. In addition, HGG used a $\sim 1".7$ beam to show that the core-to-homunculus contrast increases with decreasing wavelength between 13.1 and 8.1 μm . Thus, although the $\sim 3".5$ diameter beam size of the spectrometer includes the entire nebula, at least half of the signal shown in Figure 1 comes from a very centrally condensed core.

Although Figures 2a–2c show that η Car is extended, and that the outer contours have an oblong shape which is characteristic of other infrared maps, it is difficult to tell whether or

not the core is significantly extended with respect to a point source. Because the images were greatly oversampled and the signal-to-noise ratio of the maps is high, they are ideal candidates for image restoration. Figures 3a–3d show the result of applying a maximum-entropy image restoration algorithm to the data (Grasdalen, Hackwell, and Gehrz 1983). The restoration separates the compact core from the outer parts of the nebula, and enhances the pair of “horns” to the southeast of the core, a structure that was noted at longer wavelengths by HGG. At both 3.5 and 4.8 μm the core, although compact, is extended in the northeast-to-southwest direction at the same position angle as the double source observed by Hyland *et al.* (1979). At 10 μm (Fig. 3c), the core is much more extended than at 3.5 and 4.8 μm . This implies that much of the 10 μm emission is from different dust than that emitting at shorter wavelengths. At all wavelengths, the overall shape of the contours is very similar to the models of bipolar nebulae discussed by Morris (1981).

The infrared maps made by Hyland *et al.* (1979) resolved the core into two components separated by between 1".1 and 2".2; HGG found three core components in the 8–13 μm region each separated from the others by about 1". Figure 3d is the restored broad-band 10 μm image displayed with linearly spaced contours to show the core structure. Three core components are seen at approximately the same relative position angles as reported by HGG, but with a wider spacing. Although the results of the image restoration must be treated with some caution at the smallest spatial scales, the separation of the two brightest components is 3", almost twice the beam diameter. This is direct evidence for an expansion of the core, which might explain the recent brightening in the visible and near-infrared and our low measured value for the 10.5 μm flux.

Figure 4 shows the 3.5–4.8 μm color temperature of the central region of η Car derived assuming a blackbody emissivity law. Some of the fine structure seen in this figure (e.g., the triple peaks at 500 K) might not be real because the ratio computed at a given point depends critically upon the relative alignment of the 3.5 and 4.8 μm maps; nevertheless, the overall structure will still be meaningful. We do consider it significant that the 3.5–4.8 μm color temperature decreases rapidly beyond a radius of $\sim 2"$ from the core, yet at this radius the 10 μm flux has fallen little from its peak value. This result is consistent with, but extends, the analysis made by HGG. They showed that between 8 and 13 μm the emission from the object is primarily from silicate dust extending over a 12" \times 18" region, but with a distinctly higher temperature in the core. Consistent with the preceding discussion and the 8.1 μm map from HGG, the 4–8 μm radiation is at a higher color temperature than the silicates and must come mainly from dust within the $\sim 2"$ diameter core. Thus, we expect the spectrum shown in Figure 1 to represent primarily radiation from the core, even though our spectrometer used a beam diameter of $\sim 3".5$.

We postulate that there are two components in the dust population: a core component devoid of spectral features at a temperature ~ 500 K, and a second component, composed primarily of silicates, which is broadly distributed over about 5" around the central dusty core source and which has a range of temperatures below 500 K. (Robinson, Hyland, and Thomas 1973 also proposed a two-component model with $T_{\text{inner}} \approx 875$ K, consistent with shorter wavelength emission being dominated by hotter dust, and $T_{\text{outer}} \approx 375$ K.)

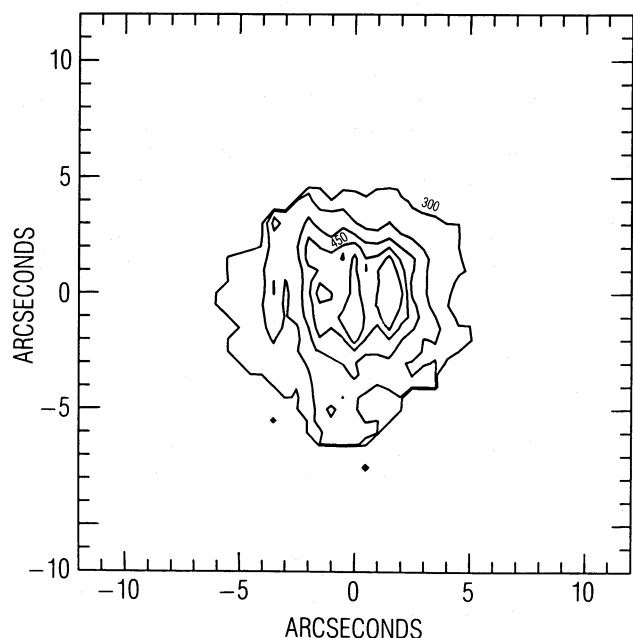


FIG. 4.—The 3.5–4.8 μm color temperature for the central region of η Car. Color temperatures were calculated assuming that the emissivity was independent of wavelength. The outer contour is 300 K, with 50 K increments to a maximum value of 500 K for three central peaks. Although some of the detailed structure (e.g., the triple 500 K peaks) may not be real because the ratio computed at a given point depends critically upon the relative alignment of the maps, the overall structure, which shows a hot core and a rapid decrease in temperature at radii greater than $2''$, is significant.

V. CONCLUSIONS

The spectrum of η Car from 4.5 to 7.5 μm has a color temperature of 375 K and is featureless, showing neither broadband nor narrow-band emission features. The upper limit to the strength of the [Ar II] 6.98 μm line of $7 \times 10^{-16} \text{ W cm}^{-2}$ is sufficiently high to allow Ar to be overabundant relative to cosmic values by a factor of ~ 100 , and is consistent with the evolved nature of the source.

Using 3.5 and 4.8 μm maps, it is shown that the dust tem-

perature is strongly peaked on a very centrally condensed core. Reasoning from the shape of the spectrum presented here and from data published elsewhere, we suggest that there are two grain populations in η Car: an extended silicate grain source and a core source which contains grains with gray emissivity in the 4–8 μm region.

Image restoration shows structures which are consistent with those seen in biconical nebulae. There is evidence for an expansion of the core at 10.5 μm which might explain the recent brightening in the visible and near-infrared and our measured low value for the 10.5 μm flux.

The authors gratefully acknowledge the assistance provided by Carl Gillespie of NASA/Ames Medium Altitude Missions Branch; NASA pilots D. Dugan, T. Raeger, P. Morris, C. Call, R. Gerdes, G. Hardy, and S. Sprague; and the invaluable ground support provided by Northrop Services, Inc. The LJO was under the direction of Paul Hagen of Teledyne Brown Engineering, and would not exist without his skill and dedication. The successful operation of an airborne observatory is always a significant challenge, and using a tropical atoll as a base further compounds the difficulties. Paul Alvarez is singled out for his extreme dedication and initiative in maintaining the airborne telescope optically, electrically, and mechanically. We would also like to thank Colonel W. Spin, Commanding Officer of the Army's Kwajalein Missile Range, and Lieutenant-Colonel Gates and Captain A. Vosburgh of the Range Operations Office for hosting the Learjet. Valuable technical support was also provided by Mike Dix, NASA/Ames, who reworked the servo system to accommodate the new telescope seal and mount; D. A. Retig of the Aerospace Corporation; D. Thornley and staff of Aeromet, Inc.; and M. Robinson of Informatics, Inc. J. A. H. and M. W. C. thank the staff and night assistants at Cerro Tololo Inter-American Observatory for their assistance, and particularly S. Schaller for his help with the fast-mapping programs. We thank D. Edelson for helping with the image enhancement software. This work was supported by National Aeronautics and Space Administration contract NAS2-12370 and by the Aerospace Sponsored Research Program in the Space Sciences Laboratory.

REFERENCES

- Aitken, D. K., and Jones, B. 1975, *M.N.R.A.S.*, **172**, 141.
 Allen, C. W. 1973, *Astrophysical Quantities* (3d ed.; London: Athlone).
 Allen, D. A., Jones, T. T., and Hyland, A. R. 1985, *Ap. J.*, **291**, 280.
 Brocklehurst, M. 1971, *M.N.R.A.S.*, **153**, 471.
 Cameron, A. G. W., and Allen, C. W. 1984, private communication.
 Gaviola, E. 1950, *Ap. J.*, **111**, 408.
 Gehr, R. D., Ney, E. P., Becklin, E. E., and Neugebauer, G. 1973, *Ap. Letters*, **13**, 89.
 Giles, K. 1977, *M.N.R.A.S.*, **180**, 57P.
 Grasdalen, G. L., Hackwell, J. A., and Gehr, R. D. 1983, in *Joint Topical Conference on Image Processing (AAS/OSA, ThB4-1)*.
 Hackwell, J. A., Gehr, R. D., and Grasdalen, G. L. 1986, *Ap. J.*, **311**, 380 (HGG).
 Hackwell, J. A., and Schweizer, F. 1983, *Ap. J.*, **265**, 643.
 Hecht, J. H., Russell, R. W., Stephens, J. R., and Grieve, P. R. 1986, *Ap. J.*, **309**, 90.
 Herschel, J. F. W. 1847, *Results of Astronomical Observations Made during the Years 1834, 5, 6, 7, 8 at the Cape of Good Hope* (London: Smith, Elder).
 Hyland, A. R., Robinson, G., Mitchell, R. M., Thomas, J. A., and Becklin, E. E. 1979, *Ap. J.*, **233**, 145.
 Joyce, R. R. 1975, *Pub. A.S.P.*, **87**, 917.
 Malin, D. 1987, *Sky and Tel.*, **73**, 14.
 Mitchell, R. M., Robinson, G., Hyland, A. R., and Jones, T. J. 1983, *Ap. J.*, **271**, 133.
 Morris, M. 1981, *Ap. J.*, **249**, 572.
 Neugebauer, G., and Westphal, J. 1968, *Ap. J. (Letters)*, **152**, L89.
 Robinson, G., Hyland, R. A., and Thomas, J. A. 1973, *M.N.R.A.S.*, **161**, 281.
 Russell, R. W. 1984, *NASA Conf. Pub. 2353*, p. 26.
 Russell, R. W., Soifer, B. T., and Willner, S. P. 1977, *Ap. J. (Letters)*, **217**, L149.
 Saari, J. M., and Shorthill, R. W. 1967, *Isothermal and Isophotic Atlas of the Moon Contours through Lunation* (NASA CR-855).
 Tielen, A. G., Allamandola, G. M., Bregman, L. T., Goebel, J., d'Hendecourt, L. B., and Witteborn, F. C. 1984, *Ap. J.*, **287**, 697.
 Warren-Smith, R. F., Scarrott, S. M., Murdin, P., and Bingham, R. G. 1979, *M.N.R.A.S.*, **187**, 761.
 Westphal, J., and Neugebauer, G. 1969, *Ap. J. (Letters)*, **156**, L45.
 Whitelock, P. A., Feast, M. W., Carter, B. S., Roberts, G., and Glass, I. S. 1983, *M.N.R.A.S.*, **203**, 385.
 Willner, S. P., Puetter, R. C., Russell, R. W., and Soifer, B. T. 1980, in *IAU Symposium 87, Interstellar Molecules*, ed. B. H. Andrew (Dordrecht: Reidel), p. 381.

MICHAEL W. CASTELAZ: Allegheny Observatory, Pittsburgh, PA 15214

JOHN A. HACKWELL, DAVID K. LYNCH, GEORGE S. ROSSANO, RICHARD J. RUDY, and RAY W. RUSSELL: The Aerospace Corporation, Space Sciences Laboratory, Mail Stop M2-266, P.O. Box 92957, Los Angeles, CA 90009